Rotational dynamics of proteins from spin relaxation rates and molecular dynamics simulations

O. H. Samuli Ollila*

Insititute of Biotechnology, University of Helsinki
(Dated: May 26, 2017)

I. INTRODUCTION

Protein conformational sampling and entropy plays significant role in protein functionality and interactions with other biomolecules. The related Protein backbone and side chains dynamics as well as protein overall brownian tumbling can be experimentally studied by using NMR relaxation experiments of backbone N-H or side chain ?? bonds [1–3]. Spin relaxation data is usually analyzed by describing the sampled bond orientations with order parameter S^2 respect to the protein reference frame and assuming that overall and internal motions are independt [2**?**]. Order parameters and timescales for overall and internal motions can be then extracted by fitting various functional forms to spin relaxation data measured with different magnetic field strengths [1, 2].

This approach has been successfully applied for large amount of proteins with isotropic shape and overall rotational diffusion [1]. The resulting order parameters and overall rotational diffusion coefficients have been used in wide range applications, including analysis of conformational entropy [**?**], binding entropy of ?? [**?**], resolving sampled structures [**?**] and validating molecular dynamics simulations [**?**].

Two different approaches have been commonly used to analyze rotational dynamics from NMR relaxation experiments. In "model free analysis" the fundamental idea is to separate interal dynamics from global rotation and assume exponential forms for rotational correlation functions. The parameters of rotational correlation functions are then fitted the experimental data to solve time scales and order parameters for different dynamical processes [**?**]. Alternative approach is to use bead models and hydrodynamical calculations to describe protein dynamics and predict spin relaxation rates [**?**]. The approaches have been successfull or several proteins, but both suffer from significant limitations which limit the general applicability [**?**]. Main practical issue in the "model free analysis" is that the amount of freen parameters to be fitted in the experiments becomes large for anitoropic proteins experiencing complex dynamics [**?**]. On the other hand, hydrodynamical calculations are sentitive for the assumptions about protein hydration shell [**?**].

Classical molecular dynamics simulations have been considered as a promising tool for interpretation of rotational motions from NMR relaxation data, because they simultaneously contain internal rotation, global browian tumbling, anisotropy and hydration shell effects [**?**]. However, practical applications have been limited by the inaccuracies in force field descriptions and available time scales in the simulations. The most used water model in rotational dynamics studies, tip3p [**?**], predicts too fast rotational diffusion [**?**]. On the other hand, very long simulations are needed to collect enough statistics to calculate rotational correlation functions from single molecules in MD simulations [**?**]. Consequnetly, protein rotational diffusion coefficients are not typically calculated from simulation data. Instead, the calculated relaxation rates are fitted to experiments by assuming an isotropic diffusion model [**?**].

In this work we overcome these issues by directly calculating diffusion coefficients from protein intertia axes. Diffusion coefficients can be then used to determine global rotational correlation functions from shorter simulations than with direct calculation. Furthermore, the oversestimated dynamics due to water model can be anisotropically corrected by scaling the diffusion coefficients with a constant factor. The usefullness of the approach is demonstrated by interpreting the spi relaxation data from aniotropic protein constructs from TonB of Helicobacteri pyroli [**?**] and Pseudomonas [**?**]. These segments are considered as vital parts related to iron transport into Gran-negative bacteria [**?**].

II. METHODS

A. Spin relaxation and rotational dynamics of molecules

Practical approaches to analyze molecular dynamics from NMR relaxation data are usually based on the connection between second order rotational correlation function $C(t)$ of N-H bond and experimentally measured spin relaxation rates R_1, R_2 and R_{NOE} through Redfield equations [4, 5]

$$R_1 = \frac{d_{\mathrm{NH}}^2 N_{\mathrm{H}}}{20}\left[J(\omega_{\mathrm{H}} - \omega_{\mathrm{N}}) + 3J(\omega_{\mathrm{N}}) + 6J(\omega_{\mathrm{N}} + \omega_{\mathrm{H}})\right]$$
$$+ \frac{(\sigma\omega_{\mathrm{N}})^2}{15}j(\omega_{\mathrm{N}}),$$

(1)

$$R_2 = \frac{1}{2}\frac{d_{\mathrm{NH}}^2 N_{\mathrm{H}}}{20}\left[4J(0) + 3j(\omega_{\mathrm{N}}) + J(\omega_{\mathrm{H}} - \omega_{\mathrm{N}}) + 6J(\omega_{\mathrm{H}})\right.$$
$$\left. + 6J(\omega_{\mathrm{N}} + \omega_{\mathrm{H}})\right] + \frac{(\sigma\omega_{\mathrm{N}})^2}{15*6}[4J(0) + 3J(\omega_{\mathrm{N}})],$$

(2)

$$R_{\mathrm{NOE}} = 1 + \frac{d_{\mathrm{NH}}^2 N_{\mathrm{H}}}{20}\left[6J(\omega_{\mathrm{N}} + \omega_{\mathrm{H}}) + J(\omega_{\mathrm{H}} - \omega_{\mathrm{N}}))\right]\frac{\gamma_{\mathrm{H}}}{\gamma_{\mathrm{N}}R_1},$$

(3)

* samuli.ollila@helsinki.fi; Department of Neuroscience and Biomedical Engineering, Aalto University

where ω_N and ω_H are the Larmor angular frequencies of ^{15}N and ^1H respectively, and N_H is the number of bound protons. Spectral density $J(\omega)$ is the Fourier transformation of the second order rotational correlation function for N-H bond

$$J(\omega) = 2 \int_0^\infty C(t) \cos(\omega t) \mathrm{d}t. \tag{4}$$

The second order rotational correlation is defined as

$$C(t) = \langle (3\cos^2 \theta_{t';t'+t} - 1)/2 \rangle_{t'}, \tag{5}$$

where average is ensemble average and θ is the angle between N-H bonds at times t' and $t'+t$. The dipolar coupling constant is given by

$$d_{NH} = -\frac{\mu_0 \hbar \gamma_H \gamma_N}{4\pi \langle r_{CN}^3 \rangle},$$

where μ_0 is the magnetic constant or vacuum permeability, $\hbar$ is the reduced Planck constant, γ_N and γ_H are the gyromagnetic constants of ^{15}N and ^1H, respectively. Average cubic length is $\langle r_{CN}^3 \rangle \approx$ and the chemical shift anisotropy is $\Delta\sigma \approx 160 * 10^{-6}$ for N-H bonds in proteins [?]. Same equations can be used, for example, to C-H bond by changing the constants related to nitrogen to the ones corresponding carbon.

Experimental spin relaxation rates of proteins are typically intepreted by assuming that the global and interal rotational dynamics are independent. The rotational correlation function for each bond can be then written as [?]

$$C(t) = C_I(t)C_O(t), \tag{6}$$

where $C_I(t)$ and $C_O(t)$ are correlation functions for internal and overall rotiations, respectively. Within this approximation the internal rotational correlation function decays to a plateau, which defines the square of order parameter respect to molecular axes S^2. Timescale for internal relaxation dynamics can be estimated by using the effective internal correlation time

$$\tau_{\mathrm{eff}} = \int_0^\infty C_I'(t) \mathrm{d}t, \tag{7}$$

where $C_I'(t) = (C_I - S^2)/(1 - S^2)$ is the reduced correlation function [?].

The global rotational dynamics for fully anisotropic molecule can be described as a sum of five exponentials [?]

$$C_O(t) = \sum_{j=1}^{5} A_j e^{-t/\tau_j}, \tag{8}$$

where time constants τ_j are related [6] to the diffusion constants around three principal axes of a molecule (D_{xx}, D_{yy} and D_{zz}) and prefactors A_j can be related to the directions of bond respect to the principal axes. The rotational diffusion

constants are defined as

$$\langle (\Delta\alpha_{t';t'+t})^2 \rangle_{t'} = 2D_{xx}t$$
$$\langle (\Delta\beta_{t';t'+t})^2 \rangle_{t'} = 2D_{yy}t \tag{9}$$
$$\langle (\Delta\gamma_{t';t'+t})^2 \rangle_{t'} = 2D_{zz}t,$$

where $\langle (\Delta\alpha_{t';t'+t})^2 \rangle_{t'}$, $\langle (\Delta\beta_{t';t'+t})^2 \rangle_{t'}$ and $\langle (\Delta\gamma_{t';t'+t})^2 \rangle_{t'}$ are mean square angle deviations of protein intertia axes.

The internal and overall correlation functions are monoexponential for proteins with isotropic overall rotational diffusion and single timescale for internal motion. The dynamics of such proteins is described with three parameters in the original "model free analysis"; internal rotational relaxation time τ_e, global rotaional relaxation time τ_c and the order parameter S^2. The values for these parameters can be then determined by fitting the Eqs. 1-8 to experimental spin relaxation data [?]. However, the amount of exponentials needed to describe correlation functions, and thus the free parameters, in such fit increases if proteins experience anisotropic overall diffusion or several internal timescales. Thus the "model free analysis" becomes less applicable for proteins with significant anisotropy or more complicated internal dynamics.

B. Rotational dynamics from molecular dynamics simulations

Classical molecular dynamics simulation gives a trajectory for each atom in a system as a function of time. These trajectories can be used to calculate rotational correlation functions for each bond from Eq. 5. The rotational correlation functions can be further used to calculate the spin relaxation times through Eqs. 1-4 and the resulting values can be compared to experimental data in order to assess simulation model quality [?] and interpret experiments [?]. However, the comparison is often complicated by the short simulation times [?] and incorrect overall rotational diffusion due to water models [?].

Here we use overall rotational diffusion constants calculated from Eq. 9 to determine the timescales of global rotational correlation function in Eq. 8. The rotational diffusion coefficients are given by a linear fit to the mean square angle deviation of intertia axes calculated from simulations (see results and discussion). Straight line has only one parameter (slope) to be fitted, in contrast to multiexponential sum in Eq. 8 with ten parameters. Thus, the calculation of timescales through overall rotational diffusion constants is numerically more robust and requires less simulation data than a direct fit of Eq. 8 to the rotational correlation function calculated from simulation. The prefactors in 8 are determined by fitting to correlation function calculated from simulations, but timescales from rotational diffusion coefficients are used. The rotational diffusion constants can be also scaled with a constant factor and new correlation functions calculated to compensate the incorrect rotational diffusion due to water model in spin relaxation rate calculations.

The analysis can be divided in essentially six steps:
1) Total rotational correlation functions $C(t)$ for protein N-H bonds are calculated from MD simulation trajectory by applying Eq. 5.

2) Rotational correlation functions for internal dynamics $C_I(t)$ are calculated from a trajectory from where the overall rotation of protein is removed.

3) The overall and internal motions are assumed to be independent and overall rotational correlation function is calculated as $C_O(t) = C(t)/C_I(t)$ according to Eq. 6.

4) The protein axes of inertia and their mean square deviations as function of time are calculated from MD simulation trajectory.

5) Rotational diffusion constants D_x, D_y and D_z are calculated by fitting a straight line to mean square angle deviations of inertia axes according to Eq. 9.

6) Timescales in Eq. 8 are calculated from diffusion constants and weighting factors A_j are determined by fitting the equation to rotational correlation functions of overall rotational motion $C_0(t)$ determined in step 3.

7) New total rotational correlation functions based on Eqs. 6 and 8 are determined as

$$C_N(t) = C_I(t) \sum_{j=1}^{5} A_j e^{-t/\tau_j}, \tag{10}$$

where internal correlation function $C_I(t)$ is taken from step 2, τ_i values from rotational diffusion constants (step 5) and prefactors A_j from step 6. The incorrect rotational diffusion due to water model can be compensated in new correlation functions at this point by scaling the rotational diffusion coefficients with a constant factor.

C. Simulation and analysis details

Simulations were ran using Gromacs 5 [7] And Amber ff99SB- ILDN [8] force field for proteins . The proteins were solvated to tip3p[9], tip4p [9] or OPC4 [10] water models. NMR structures from [?] and [11] are used as initial structure for PaTonB and HpTonB-92, respectively. Temperature was coupled to desired value with v-rescale thermistat [12] and pressure was isotropically set to 1 bar using Parrinello-Rahman barostat [13]. Timestep was 2 fs, Lennart-Jones interactions were cut-off at 1.0 nm, PME [14, 15] was used for electrostatics and LINCS was used to constraint all bond lengths [16]. Simulation trajectory and related files are available at [??]. The simulated systems are listed in Table I

Rotational correlation functions are calculated with *gmx rotacf* and overall rotation for $C_I(t)$ calculation is removed by using fit option in *gmx trjconv* grom Gromacs package [17]. Inertia axes of protein for rotational diffusion calculation are calculated with *compute_inertia_tensor* from MDTraj python library [18]. For spectral density calculation a sum of 471 exponentials having correlation times from 1 ps to 50 ns with logarithmic spacing

$$C_N(t) = \sum_{i=1}^{N} \alpha_i e^{-t/\tau_i} \tag{11}$$

were fitted to the new correlation function calculated from

Eq. 10 by using the *lsqnonneg* routine in MATLAB [19]. The Fourier transform is then calculated by using analytical function for the sum of exponentials

$$J(\omega) = 4 \sum_{i=1}^{N} \alpha_i \frac{\tau_i}{1 + \omega^2 \tau_i^2}. \tag{12}$$

Similar approach is used previously for lamellar systems in combination with solid state NMR experiements [20, 21].

III. RESULTS AND DISCUSSION

A. Global rotational dynamics of protein

Rotational diffusion coefficients are calculated according to Eq. 9 by fitting a linear slope to the mean square angle deviations of protein intertia axes as a function of time. The mean square angle deviations and linear fits are exemplified for different simulations of PsTonB in Fig. 1. The overall rotational dynamics can be considered to be diffusive with a good approximation; the data plotted with log-log scale in Fig. 8 reveal a weakly subdiffusive region only below 0.12 ns. Also visual inspection of the data plotted with linear scale in Fig. 1 reveals very linear behaviour with lag times less than one hundredth of the total simulation length, which is expected to give good statistics for rotation of single molecules in MD simulations [?]. The deviations from linear behaviour seen with longer timescales than this are considired to arise from insufficient statistics. Thus, the diffusion coefficients are calculated by fitting linear line to the mean square angle deviations with lag times less than one hundreth of the total simulation lenght.
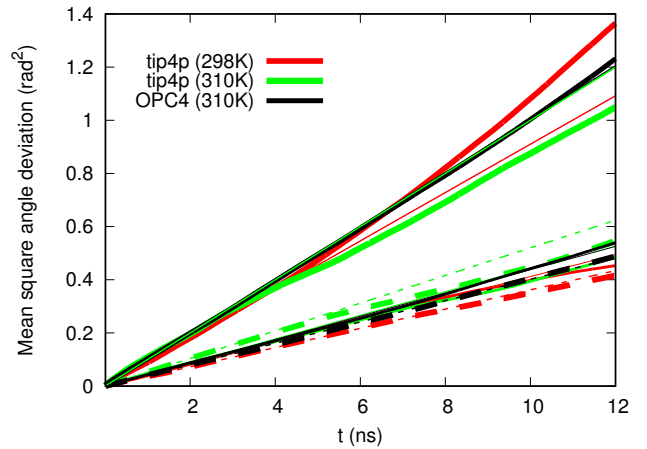

FIG. 1. The intertia tensor angles as a function of time and mean square angular deviations for PsTonB simulation with OPC water model.

The results for diffusion constants from different simulations shown in Table I are in line with previous results from experiments [?] and simulations [?] for more isotropic

TABLE I. Simulated systems and rotational diffusion coefficients (rad$^2 \cdot 10^7$/s) calculated from simulations.

Protein	Water model	T (K)	t_{sim} (ns)	t_{anal} (ns)	D_{xx}	D_{yy}	D_{zz}	$D_{||}/D_+$	D_{av}	files
PaTonB	tip4p	298	400	390	1.81 ± 0.01	2.06 ± 0.03	4.55 ± 0.03	2.35 ± 0.04	2.80 ± 0.02	[?]
PaTonB	tip4p	310	400	390	2.60 ± 0.02	2.22 ± 0.05	5.0 ± 0.1	2.07 ± 0.09	3.26 ± 0.07	[?]
PaTonB	OPC4	310	1200	1190	2.01 ± 0.01	2.19 ± 0.01	5.01 ± 0.03	2.39 ± 0.02	3.07 ± 0.01	[?]
HpTonB-92	tip3p	310	570	370	8.25 ± 0.05	7.67 ± 0.06	15.9 ± 0.3	1.99 ± 0.06	10.6 ± 0.2	[?]
HpTonB-92	tip3p	303	800	790	6.24 ± 0.02	7.04 ± 0.03	11.9 ± 0.2	1.80 ± 0.03	8.40 ± 0.07	[?]
HpTonB-92	tip4p	310	470	370	3.6 ± 0.1	3.24 ± 0.01	6.3 ± 0.3	1.8 ± 0.1	4.4 ± 0.2	[?]
HpTonB-92	tip4p	303	400	200	2.7 ± 0.1	2.71 ± 0.02	5.6 ± 0.5	2.1 ± 0.2	3.7 ± 0.2	[?]
HpTonB-92	OPC4	310	800	790	2.85 ± 0.01	2.70 ± 0.01	5.56 ± 0.01	2.00 ± 0.01	3.70 ± 0.01	[?]

proteins. As expected, rotational diffusion is faster in simulations with higher temperature or smaller protein. Also the larger diffusion constants for simulations with tip3p are expected due to the low viscosity of the model [?].

Inclusion of rotational diffusion coefficients in N-H bond rotational correlation functions is exemplified in in Fig. 2 for residue 331 located in alpha helix of PaTonB protein. The same analysis is performed also to other bonds and the resulting correlation functions are used to calculate spin relaxation rates. As expected, the N-H bond correlation functions calculated from original MD trajectories shown in Fig. 2 A) decay to fluctuate approximately around zero after $\sim$20ns. Fluctuations from ideal relaxation behaviour begin already close to one hundredth of total simulation time (approximately 4-12ns for the studied systems), which is expected to be the limit for good statistic for rotational dynamics analyzed from single molecule MD simulation [?]. Internal correlation functions, calculated from trajectory with overall protein rotation removed, in Fig. 2 B) show rapid decay to a plateau value, which defines the square of the order parameter S^2. The global rotational correlation functions calculated as $C_O(t) = C(t)/C_I(t)$ are shown in Fig. 2 C).

Overall rotational correlation functions were fit to Eq. 8, where timescales for anisotropic rotation [6] were determined by using rotational diffusion constants from Table I, to determine the prefactors A_j for all residues. Resulst for such fit are exemplified with dashed lines in Fig. 2 C) for residue 331 of PsTonB. The prefactors, global rotational timescales and correlation functions for internal relaxation were used to determine new correlation function $C_N(t) = C_I(t) \sum_{j=1}^{5} A_j e^{-t/\tau_j}$, where internal correlation comes directly from MD simulation and global rotational correlation function from diffusion coefficients calculated from MD and Eq. 8. The new correlation functions are exemplified with dashed lines in Fig. 2 A) for residue 331 of PsTonB.

B. Global rotational dynamics in simulations and experiments

These issues have been typically overcame by introducing isotropic rotational diffusion term in the correlation functions [?] or comparing order parameters instead of spin relaxation rates [?]. These approaches are not, however, useful for anitropic proteins and order parameter comparison is not direct
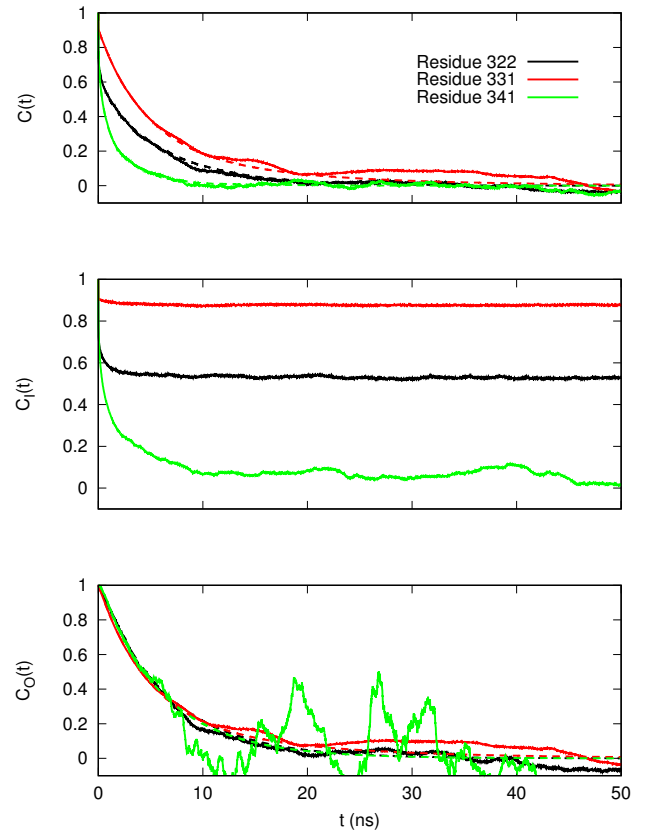

FIG. 2. Example correlation functions for residue 331 of PsTonB calculated from MD simulations with different water models. A) total correlation functions $C(t)$ calculated from MD simulation (solid lines) and new correlation functions determined from Eqs. 6 and 8 by using rotational diffusion constants and fitted prefactors (see section II B) (dashed lines), B) correlation function for internal motions and C) correlation function for overall motions determined from Eq. 6 ($C_O(t) = C(t)/C_I(t)$) (solid lines) and fits to Eq. 8.

comparison between simulations and experiments in the case of freely rotating molecules.

Spin relaxation rates were calculated from MD simulations by using new correlation functions, where global rotational

dynamics is described by Eq. 8 with timescales from diffusion constants in Table I and prefactors fit to the MD simulation data. The results for PaTonB and HpTonB simulations with different water models are shown in Figs. 3 and **??**, respectivelty.
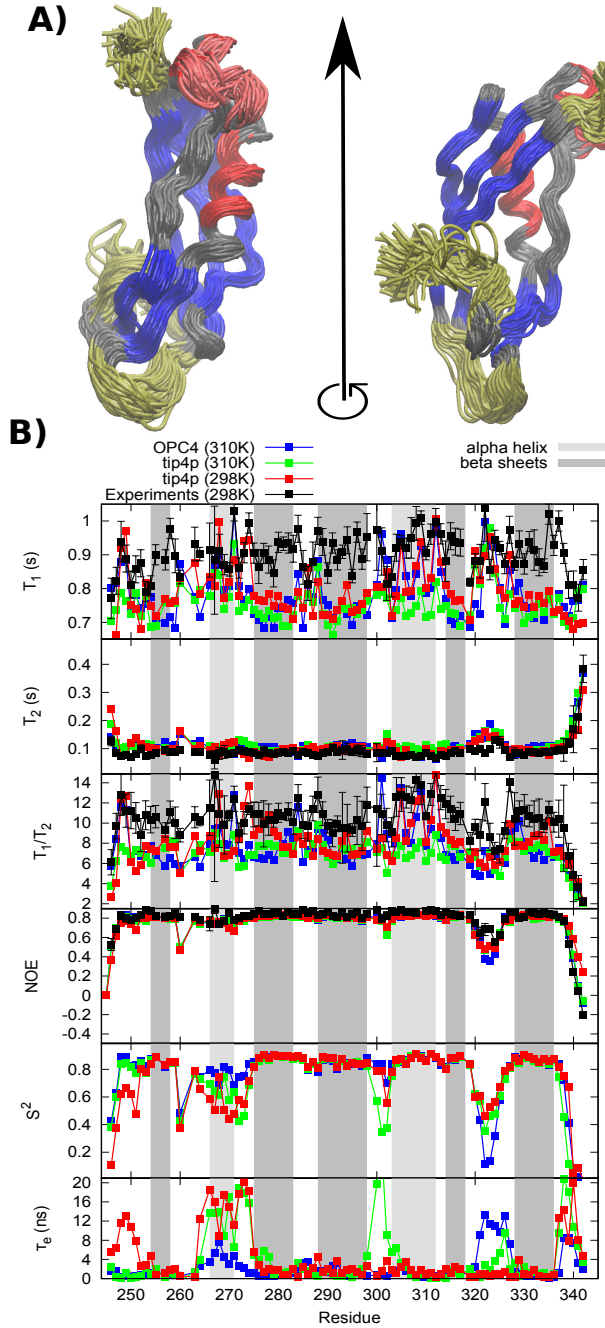

FIG. 3. A) Structures sampled by PsTonB from MD simulations (100 structures from 400ns long trajectory). Alpha helixces are shown with red, beta sheets with blue and residues 246-251, 320-326 and 338-342 with increased internal dynamics are colored yellow. Alphahelix sampling between two orientations (residues 266-270) is shown with pink in left column. B) Spin relaxation rates, order parameters and effective internal correlation times from experiments and simulations.
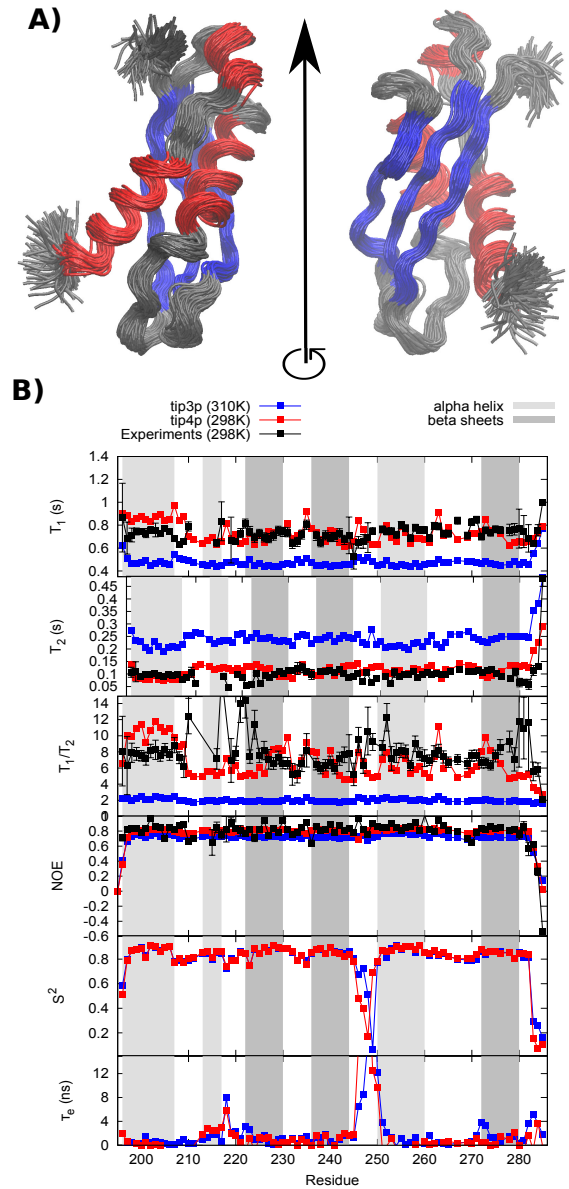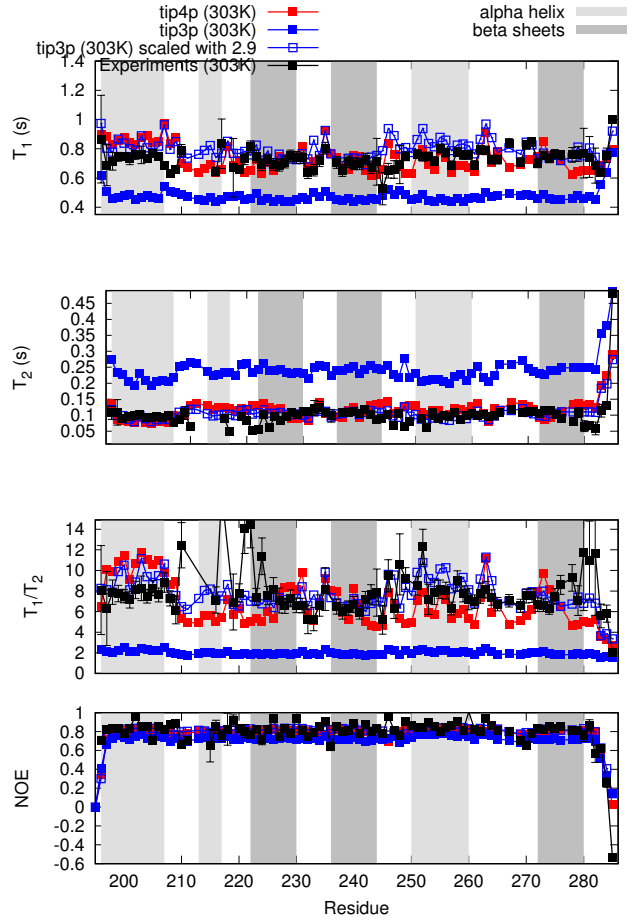

FIG. 4. Relaxation parameters for HpTonB short construct from experiments and simulations with Amber-ildn and different water models

For PaTonB T_1 and T_1/T_2 ratio are slightly underestimated systemically in all simulations. For HpTonB tip4p gives good agreement with experiments but tip3p results are significantly off. Underestimation of T_1/T_2 ratio suggests that the global rotational diffusion is overestimated in simulations [**?**]. Thus, we tested if scaling of diffusion coefficients with constant factor gives better agreement with experiments. Rotational diffusion coefficients for PaTonB simulation with tip4p and HpTonB simulation with tip3p were first divided by factors 1.2 and 2.9, respectively. Then, the new correlation functions $C_N(t)$ were calculated by using timescales determined from scaled diffusion constants and prefactors from the fit to the overall correlation functions. The spin relaxation results from these correlation functions are shown in Figs. 5 and 6 for PsTonB and HpTonB, respectively, are in good agreement

cesses experienced by different residues can be done by analysing timescales which leads in simulation model to the spin relaxation rates in agreement with experiments. Prefactors from Eq. **??** fitted in rotational correlation functions in agreement with spin relaxation data are shown in Fig 7 for different residues in PsTonB. Residue 331 represents the last alpha helix before C terminus and its rotational relaxation is mostly dominated by relaxations with timescales ~5.5 ns and ~8 ns, which arise from global rotation of protein an only small fraction of relaxation arises from fast internal motions, in accordance with large order parameter value (??). Relaxation of residue 322 is also dominated by relaxation processes with timescale around ~8 ns, but fast motions related to internal protein dynamics are more significant than for alpha helix residue 331. This explains the low order parameter (??) measured small NOE and large T_2 relaxation times values shown in Fig. **??**. Rotational dynamics of residue 341 located in N terminus is dominated by the fast motions related to the internal protein relaxation, as expected from the low order parameter. The contribution from timescales close to ~13 ns are probably related to slower conformational sampling of the N terminus, which is also seen in sampled conformations and large effective correlation times in Fig. **??**.
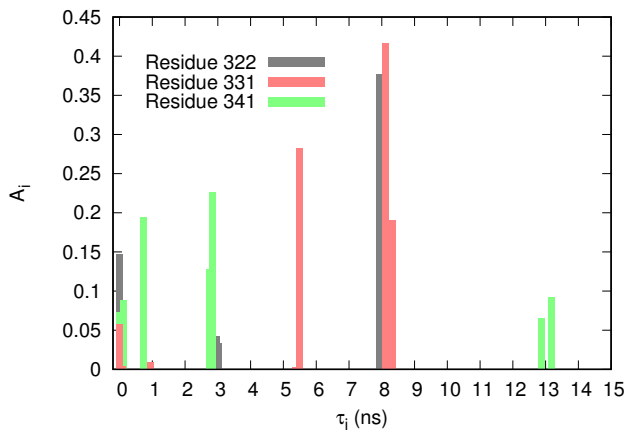

FIG. 7. Prefactors A_i corresponding different timescales τ_i in Eq.**??** resulting from a fit in correlation functions giving good agreement with spin relaxation rates in experimetns for PsTonB.

In addition, low order parameters and larger effective correlation times are observed for PsTonB residues 260-274 and 300-303 in Fig. 3 B). For residues 260-274 this can be explained by two different orientations sampled by alpha helix on that region, as highlighted with pink in Fig. 3 A). This explains also the lower resolution in NMR spectra observed for this and similar region in HpTonB structures [**?**]. Low order parameters and large effective correlation times between residues 300-303 are not seen in spin relaxation data, thus it is not clear if these arise from simulation artefact.

Spin relaxation rate deviations from baseline are observed only few residues in terminal ends for HpTonB-92 as seen in Fig. **??**. This is the case also in simulations, except that the N terminus flexibility seems to be somewhat overestimated and low order parameters and long effetive correlation times are also observed for residues 245-250. The latter observation probably arises (at least partly) from simulation artefacts because deviation form experimental relaxation data is relatively large for these residues. More detailed discussion together with longer HpTonB construct is presented elsewhere [**?**].

IV. CONCLUSIONS

Rotation of protein intertia axes is observed to experience linear diffusion behaviour and overall diffusion component of rotational correlation functions of individual N-H bonds can can be successfully fitted to the model assuming anitropic diffusion for whole molecule.

Rotational diffusion of whole molecules is overestimated by a factor of ~3 in simulations with tip3p water, in agreement with previous studies [**?**]. The simulations with tip4p and opc4 water models give more realistic diffusion coefficients, which overestimate diffusion only with factors ~1-1.2.

The overstimated overall diffusion coefficient can be corrected post-simulationally to compare internal dynamics and order with experiments.

The presented methodology can be used to interpret spin relaxation experiments by using MD simulations [**?**] and asses the quality of protein force fields against NMR experiments. The presented scaling of overall anisotropic diffusion allows this also for simulations with incorrect rotational diffusion due to water models, which is the case in simulations with tip3p.

[1] V. A. Jarymowycz and M. J. Stone, Chemical Reviews **106**, 1624 (2006).

[2] D. Korzhnev, M. Billeter, A. Arseniev, and V. Orekhov, Progress in Nuclear Magnetic Resonance Spectroscopy **38**, 197 (2001).

[3] .

[4] A. Abragam, *The Principles of Nuclear Magnetism* (Oxford University Press, 1961).

[5] L. E. Kay, D. A. Torchia, and A. Bax, Biochemistry **28**, 8972 (1989).

[6] $\tau_1 = (4D_{xx} + D_{yy} + D_{zz})^{-1}$, $\tau_2 = (D_{xx} + 4D_{yy} + D_{zz})^{-1}$, $\tau_3 = (D_{xx} + D_{yy} + 4D_{zz})^{-1}$, $\tau_4 = [6(D + (D^2 - L^2)^{-1/2}]^{-1}$, $\tau_5 = [6(D - (D^2 - L^2)^{-1/2}]^{-1}$, $D = \frac{1}{3}(D_{xx} + D_{yy} + D_{zz})$ and $L^2 = \frac{1}{3}(D_{xx}D_{yy} + D_{xx}D_{zz} + D_{yy}D_{zz})$.

[7] M. J. Abraham, T. Murtola, R. Schulz, S. Pll, J. C. Smith,

B. Hess, and E. Lindahl, SoftwareX **12**, 19 (2015).

[8] K. Lindorff-Larsen, S. Piana, K. Palmo, P. Maragakis, J. L. Klepeis, R. O. Dror, and D. E. Shaw, Proteins: Structure, Function, and Bioinformatics **78**, 1950 (2010).

[9] W. L. Jorgensen, J. Chandrasekhar, J. D. Madura, R. W. Impey, and M. L. Klein, J. Chem. Phys. **79**, 926 (1983).

[10] S. Izadi, R. Anandakrishnan, and A. V. Onufriev, The Journal of Physical Chemistry Letters **5**, 3863 (2014).

[11] A. Ciragan, A. S. Aranko, I. Tascon, and H. Iwa, Journal of Molecular Biology **428**, 4573 (2016).

[12] G. Bussi, D. Donadio, and M. Parrinello, J. Chem. Phys. **126** (2007).

[13] M. Parrinello and A. Rahman, J. Appl. Phys. **52**, 7182 (1981).

[14] T. Darden, D. York, and L. Pedersen, J. Chem. Phys. **98**, 10089 (1993).

[15] U. L. Essman, M. L. Perera, M. L. Berkowitz, T. Larden, H. Lee, and L. G. Pedersen, J. Chem. Phys. **103**, 8577 (1995).

[16] B. Hess, J. Chem. Theory Comput. **4**, 116 (2008).

[17] M. Abraham, D. van der Spoel, E. Lindahl, B. Hess, and the GROMACS development team, *GROMACS user manual version 5.0.7* (2015).

[18] R. T. McGibbon, K. A. Beauchamp, M. P. Harrigan, C. Klein, J. M. Swails, C. X. Hernández, C. R. Schwantes, L.-P. Wang, T. J. Lane, and V. S. Pande, Biophysical Journal **109**, 1528 (2015).

[19] .

[20] A. Nowacka, N. Bongartz, O. Ollila, T. Nylander, and D. Topgaard, J. Magn. Res. **230**, 165 (2013).

[21] T. M. Ferreira, O. H. S. Ollila, R. Pigliapochi, A. P. Dabkowska, and D. Topgaard, J. Chem. Phys. **142**, 044905 (2015).
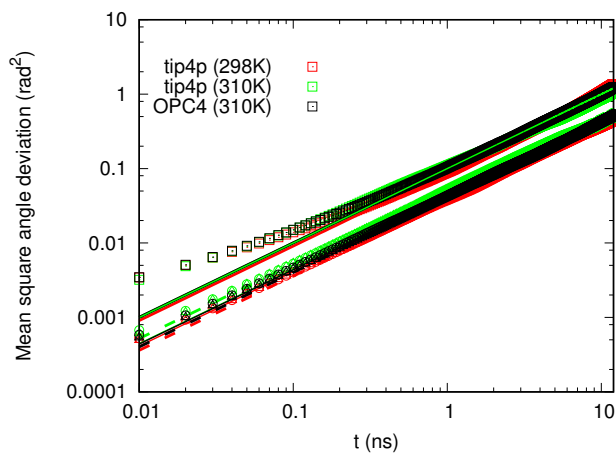
SUPPLEMENTARY INFORMATION

FIG. 8. The intertia tensor angles as a function of time and mean square angular deviations for PsTonB simulation with OPC water model.